Bridge Structures 10 (2014) 43–52
DOI:10.3233/BRS-140073
IOS Press

High temperatures and bridges: Transverse stiffeners in steel girder fire performance

J.D. Glassman* and M.E.M. Garlock
Princeton University, Princeton, NJ, USA

Abstract. Vehicular accidents involving tanker trucks may initiate devastating fires that can cripple a steel plate girder bridge. An observation of web shear buckling in one case study leads to a discussion on the existing understanding of this phenomenon. A closer look at the contribution of the transverse stiffeners to postbuckling shear capacity focuses on the effects of utilizing diagonal orientations of the stiffeners, as well as providing thermal insulation for the stiffeners alone. It was found that the diagonal stiffener models do not offer much improvement to the postbuckling shear strength compared to the use of the traditional vertical intermediate stiffener. Given the complexity of attaching a diagonal stiffener, it appears that the vertical stiffener is the better option. Further, providing fire resistance solely for the stiffeners was found to offer a minimal increase in the postbuckling shear strength at elevated temperatures.

Keywords: Bridge fire, transverse stiffener, web shear buckling, postbuckling

1. Introduction

Fire loading on highway bridges remains a real yet poorly understood threat to our transportation infrastructure. Fires that may affect bridges can come from various sources, but a potentially disastrous threat exists with vehicular fires. Of particular concern are accidents involving tanker trucks, which can tow large volumes of combustible fuels, such as gasoline and diesel, and have resulted in fiery infernos that have caused irreparable damage and catastrophic failure to numerous bridges throughout the US [10].

Steel plate girder bridges are especially susceptible to fire damage due to the significant loss of steel strength as temperatures increase. The Eurocode material model for carbon steel predicts a major loss of strength for steel temperatures increasing above 400°C, with zero mechanical performance expected at 1200°C [8]. Fires involving the ignition of hydrocarbon fuels hauled by a tanker truck can be classified as liquid pool fires, which are characterized by their fast burning rates, rapid growth phases, and large radiation loadings for pool fires with diameters greater than 1 meter [11, 16]. Temperatures generated from these liquid pool fires can be in excess of 1000°C [11], and this coupled with the potentially long burn time implies that these fires can cause significant damage if they occur near or beneath a steel plate girder bridge.

The National Fire Protection Association (NFPA) has recognized the threat that fires may pose to bridge infrastructure and stipulates that elevated temperature loading should be considered in the design, but the guidance offered is neither rigorous nor extensive. Sections 6.5 and 6.6 of the NFPA 502 document require that a standpipe be placed for the bridge if a water source is not available within 400 feet and that critical structural elements of the bridge are protected from fire [17].

*Corresponding author. J.D. Glassman, Princeton University, Princeton, NJ, USA. E-mail: jdglassm@princeton.edu.

What these critical structural elements are and how to protect them are questions currently being investigated in bridge fire research.

In this paper, web shear buckling is used as a metric for gauging the fire performance of steel plate girder bridges. As temperatures increase, the susceptibility of the slender web to shear buckling increases and potentially initiates failure propagation in the structural system. The vertical transverse stiffeners, whose spacing plays a critical role in the development of web shear buckling capacity, are studied to determine how they may assist in increasing the postbuckling shear strength at elevated temperatures.

2. Background

2.1. Case studies

Arguably one of the most catastrophic bridge fires in the US to date occurred in San Francisco, CA on April 29th, 2007. A tanker truck transporting approximately 8600 US gallons of gasoline was speeding through a 50 mph zone within the I-80/I-580/I-880 interchange (colloquially known as the MacArthur Maze) when it overturned and its combustible cargo caught fire beneath a steel plate girder bridge carrying the I-580 [10]. Two spans of the I-580 overpass collapsed approximately 22 minutes after the fire initiated, and the speed at which this collapse occurred challenges even the best of fire response times. The MacArthur Maze lies at the eastern terminus of the San Francisco-Oakland Bay Bridge and is the chief collector/distributor of vehicular and cargo traffic traveling between San Francisco and the eastern Bay Area communities. In addition to the $9 million spent by the federal government to repair and rebuild the damaged interchange, the resulting closure of a portion of this interchange complex resulted in an estimated $6 million per day economic loss to the San Francisco Bay Area [6, 10].

On January 5th, 2002, a tanker truck traveling northbound on the I-65 and hauling approximately 9,900 US gallons of gasoline was cut off by a passenger vehicle attempting to reach an exit, causing the truck to swerve and crash adjacent to the southbound I-65 overpass [20]. A two-part liquid pool fire was initiated – an *unconfined pool fire*, which resulted from fuel that spilled onto the roadway from the damaged tanker, and a *confined pool fire* that was fed by the gasoline remaining in the damaged tanker. These two components of the tanker fire can be seen in Fig. 1.

Despite the fire's proximity to the bridge, the simply supported steel plate girders did not collapse [20]. The girder closest to the fire experienced the most significant damage, with an approximately 2.5 meter vertical sag after the fire was extinguished [20]. Figure 2a shows the relative deflection of the undamaged girder located furthest from the fire with respect to the heavily damaged girder that experienced the brunt of the fire loading.

Another interesting aspect of this fire was the occurrence of web shear buckling due to the high temperatures experienced by the bridge. Figure 2b shows diagonal buckles that formed between the locations of vertical transverse stiffeners. The presence of these diagonal buckles implies that web shear buckling due to elevated temperatures did occur. This observation is a key motivator for the current work carried out to characterize this buckling phenomenon at high temperatures.

2.2. Web shear buckling

The postbuckling strength of a steel web plate subjected to pure shear loading has traditionally been characterized by its ability to form a diagonal tension field. The Basler model was the first theory known to have been proposed to analytically classify the postbuckling strength of steel plate girder webs under pure shear [5, 27]. The underlying principle behind this diagonal tension field model is that once the web plate loaded in pure shear has reached its elastic critical buckling stress, τ_{cr}, the diagonal compressive stresses in the web can no longer increase, thus any postbuckling strength is attributed to the stable formation and growth of the diagonal tension field. This restriction on the compressive stresses beyond elastic critical buckling is a fundamental assumption dating back to the 1931 work conducted by Wagner [13, 25].

The Basler-Thürlimann solution was formulated based on the assumptions of the diagonal tension field model and provides an analytical solution for the value of the ultimate shear buckling stress, τ_u [5, 27]:

$$\tau_u = \tau_{cr} + \sigma_{yw}\left(1 - \frac{\tau_{cr}}{\tau_{yw}}\right)\left(\frac{\sin\theta_d}{2 + \cos\theta_d}\right) \qquad (1)$$

σ_{yw} is the tensile yield strength of the web, τ_{yw} is the shear yield strength of the web (computed as $0.6\sigma_{yw}$ [1]), θ_d is the angle of the panel diagonal, and τ_{cr} is the elastic critical buckling stress for a rectangular plate. The classical analytical solution for τ_{cr} is [13, 22, 27]:

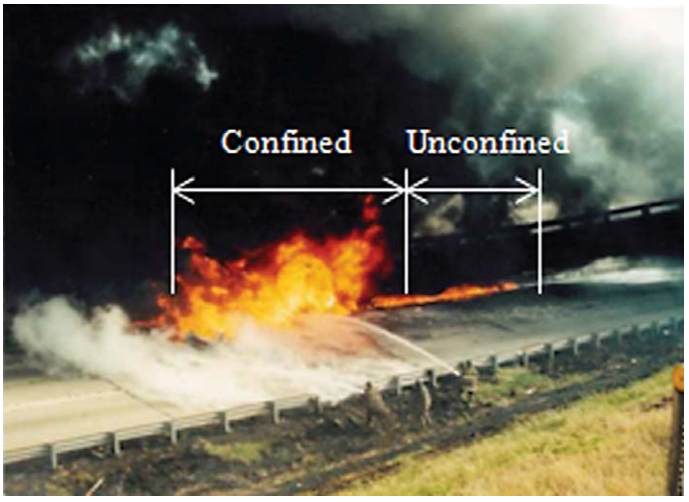

Fig. 1. Photo of the tanker truck fire (time stamp unknown). The confined pool fire exists beneath the taller flame heights, while the unconfined pool fire exists where the smaller flames extend out from the confined pool fire. Courtesy of the Alabama Department of Transportation (DOT).

Fig. 2. From left to right, (a) underside damage to the bridge, and (b) observation of web shear buckling near the column support. Photos courtesy of the Alabama DOT.

$$\tau_{cr} = k\frac{\pi^2 E}{12\left(1-\nu^2\right)\left({}^{D}/_{t_w}\right)^2} \tag{2}$$

where D is the depth of the plate, t_w is its thickness, E is Young's Modulus, ν is Poisson's ratio, and k is the shear buckling coefficient that is a function of the span (a)-to-depth ratio, a/D. For a simply supported rectangular web plate, k can be calculated as [12, 13, 22]:

$$k = 4.00 + \frac{5.34}{\left({}^{a}/_{D}\right)^2} \quad \text{for } a/D < 1 \tag{3a}$$

$$k = 5.34 + \frac{4.00}{\left({}^{a}/_{D}\right)^2} \quad \text{for } a/D \geq 1 \tag{3b}$$

In situations where $\tau_{cr}>0.8\tau_{yw}$, the τ_{cr} in equation (1) is recommended to be replaced with the inelastic buckling stress $\tau_{cr,i}$ [5, 27]:

$$\tau_{cr,i} = \sqrt{0.8\tau_{cr}\tau_{yw}} \quad \text{for } 0.8\tau_{yw} \leq \tau_{cr} \leq 1.25\tau_{yw} \tag{4}$$

For the purpose of this particular study, only simply supported web plates will be analyzed. The Basler-Thürlimann solution presented in equation (1) was predicated on the notion of a web plate idealized with

simply supported boundary conditions for the flanges and the vertical transverse stiffeners. Work carried out by Lee et al. [12] has also classified values for k for web plates supported by flanges with thickness t_f, and future research related to web shear buckling at elevated temperatures will include the contributions of the flanges to the ultimate shear buckling strength.

3. The finite element (FE) model

3.1. Geometry, material, and boundary conditions

Four FE models were developed for the current transverse stiffener study. The dimensions and ambient temperature material properties were based on a design example provided by the National Steel Bridge Alliance for a three-span continuous straight composite I-girder [2]. The depth, D, and web thickness, t_w, used were 1.75 meters and 0.014 meters, respectively. The length, a, of the web plate was 5.25 m. For the web plate shown in Fig. 3(a), this implies that the span-to-depth ratio, a/D, was 3.0. It should be noted that composite action was not considered – only the web plate subjected to a pure shear loading was modeled for the current study.

At ambient temperature (20°C), Young's Modulus, E, was assumed to be 2e11 N/m^2 and the yield stress, σ_{yw}, was 345 MPa. For the FE model shown in Fig. 3(b) that included a vertical transverse stiffener, the width and thickness of the stiffener, taken directly from the design example, were 0.130 meters and 0.013 meters, respectively. The material properties for the stiffeners were the same as for the web plate. For the FE models shown in Fig. 3(c) and (d) that employ a diagonal stiffener, the same width and thickness as that of the vertical stiffener are used. Eurocode reduction factors E and σ_{yw} were used to account for the steel softening and losing strength as the temperatures increased [8].

The three-sided sided shear loading shown for all models in Fig. 3 is similar to the loading pattern shown in previous studies [12–14, 23, 24]. The unloaded side (side ❶ in Fig. 3) is kinematically constrained in the vertical direction. The web plate is assumed to be simply supported on all four edges. Sides ❶ and ❷ correspond with the location of vertical transverse stiffeners, which in this case are idealized as simple supports based on previous studies [12, 13, 27]. The web-flange juncture, represented by sides ❸ and ❹ in Figure 3, is also idealized as simply supported to be consistent with the Basler-Thürlimann solution presented in equation (1). The simply supported boundary conditions for all four edges are listed in Table 1, where a * represents a restrained degree of freedom (DOF). U_x, U_y, and U_z are translational DOFs in the x, y, and z directions, respectively. UR_x, UR_y, and UR_z are the rotational DOFs about the x, y, and z axes.

In addition to the simply supported boundary conditions for sides ❶, ❷, ❸, and ❹ shown in Fig. 3, boundary conditions were set for the stiffeners shown in Figs. 3b–d based on the AASHTO LRFD Bridge Design Specifications [3]. Section 6.10.11.1 of these specifications requires that stiffeners not used as connection plates should have a tight fit or be attached to the compression flange, but are not required to be in bearing with the tension flange. For this study, it was assumed that the stiffener was not used as a connecting plate for diaphragms or cross-frames, therefore the stiffener was modeled to not be attached to the top flange. This assumption is valid because this study's purpose is to investigate the impact of adding a stiffener to a web plate that has already been designed for $a/D = 3.0$. For the VS model in Fig. 3b, the simply supported "Stiffener" boundary condition listed in Table 1 is provided at the bottom of the stiffener. Since the flanges are not explicitly modeled, instead being treated as simple supports, the portion of the transverse stiffener that must be attached to the compression flange is similarly provided simple supports. For the diagonal stiffeners, no boundary conditions were assumed for the edges of the stiffener closest to the top and bottom flange due to the assumed complexity of attaching a diagonal stiffener to a joint where a vertical stiffener and flange already intersect.

A tie constraint [7] was employed to connect both the vertical and diagonal stiffeners to the web plate. Section 6.10.11.1 of the *Bridge Design Specifications* specifies the distance between the end of the web-to-stiffener weld (the tie constraint in the FE model) and the near edge of the adjacent web-to-flange weld (sides ❸ and ❹ in the FE model) as being greater than $4t_w$ and less than the smaller of $6t_w$ or 4.0 inches (approximately 0.10 meters) [3]. The length of the web-to-stiffener weld used for the vertical transverse stiffener was 1.63 meters, shown in Fig. 3(e). For the diagonal stiffener, in order for the web-to-stiffener weld to maintain the proper distance from the simple supports modeling the vertical transverse stiffeners at span, a, of 5.25 meters (sides ❶ and ❷ in Fig. 3) and the top and bottom flanges (sides ❸ and ❹ in Fig. 3), the inclination of the diagonal stiffener must be taken into account. Figure 3(f) shows the length of the web-to-stiffener weld selected for the diagonal stiffener. Due to the inclination, in order to

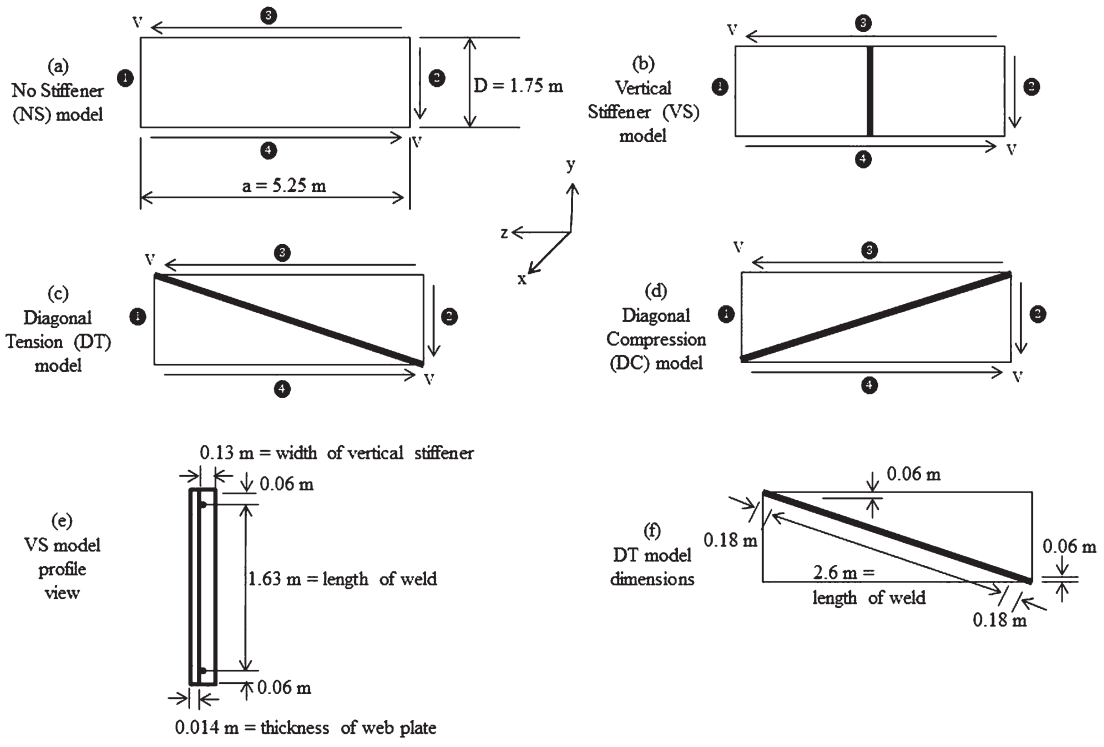

Fig. 3. Schematics of the simply supported rectangular web plates studied in this paper.

Table 1
Simply supported boundary conditions corresponding to Fig. 3

	Translation			Rotation		
	U_X	U_Y	U_Z	UR_X	UR_Y	UR_Z
❶	x	x	X	x		x
❷	x		x	x		x
❸	x		x	x	x	
❹	x		x	x	x	
Stiffener	x		x	x	x	

satisfy the distance constraint of section 6.10.11.1, the diagonal weld (tie constraint in the FE model) was specified as 2.6 m long, with 0.18 m of unwelded length at either end closest to the corners of the web plate. 0.18 m was chosen because the vertical clearance from the initiation of the web-to-diagonal-stiffener weld satisfies the distance constraint of the *Specifications* [3].

The primary motivation for investigating diagonal orientations of the stiffeners was to further probe the mechanics of web shear buckling. Of particular interest to the authors was the contribution of the compressive stresses to the postbuckling shear strength of the web plate. The fundamental assumption that the compressive stresses cease to increase beyond elastic critical shear buckling [25] has been challenged over the past several years by numerous authors [15, 18, 19, 26]. Employing diagonal stiffeners in both the tension field and compressive stresses directions offered an interesting opportunity to further explore the hypothesized contributions of the compressive stresses in the postbuckling range.

3.2. Mesh convergence study

The mesh densities for the four FE models studied in this paper are shown in Fig. 4. An eigenvalue extraction analysis was carried out at 20°C for the web plate shown in Fig. 4(a) to determine the mesh density. This

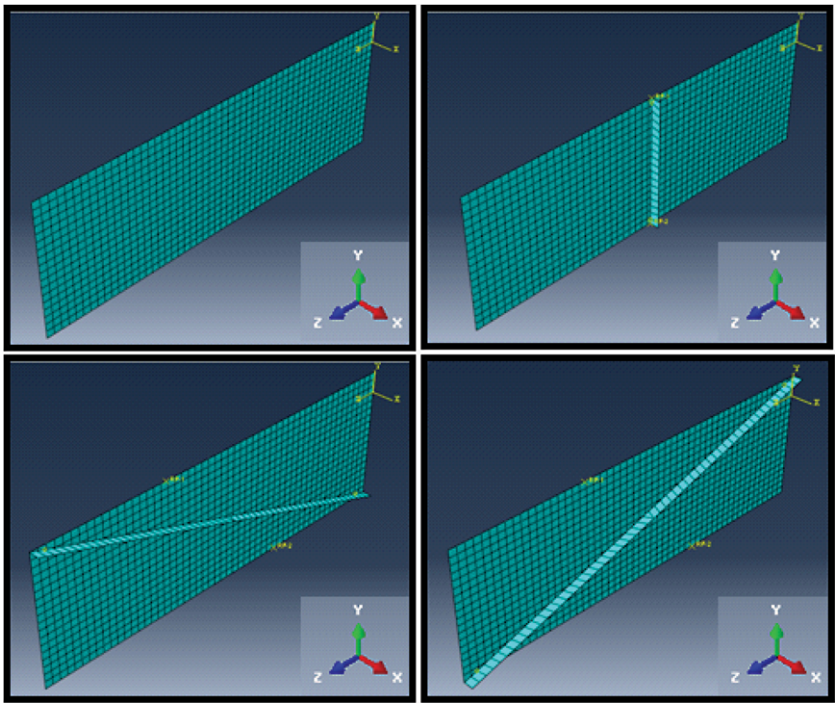

Fig. 4. Clockwise from top left, simply supported web plate with (a) a/D = 3.0, (b) intermediate vertical transverse stiffener placed such that there are two web sections with a/D = 1.5, (c) stiffener oriented diagonally parallel to the compressive stresses, and (d) stiffener oriented diagonally parallel to the tension field. The loading pattern is the same as Fig. 3.

analysis is computationally less expensive than the full nonlinear postbuckling analysis and is thus preferred for the mesh convergence study [21]. The S4 element, which is characterized as a fully integrated, general-purpose, finite-membrane-strain shell element [7], was selected. Percent errors between the elastic shear buckling stress, τ_{cr}, computed from Equation (2) and the values obtained numerically were recorded for various mesh refinements in order to track the optimization of the mesh. A mesh with 954 elements and a percent error

Table 2
Temperature dependent elastic critical shear buckling stress, τ_{cr}, values and performance ratios for the four FE models studied

Model	T (°C)	τ_{cr} (N/m^2)			Performance ratios		
		FE model		Theoretical (TH)	FE vs. TH		P vs. UP
		UP	P		UP/TH	P/TH	P/UP
No Stiffener (NS) $a/D = 3.0$	20	6.75E+07	n/a	6.56E+07	1.03	n/a	n/a
	400	4.73E+07	n/a	4.59E+07	1.03	n/a	n/a
	700	8.78E+06	n/a	8.53E+06	1.03	n/a	n/a
	1000	3.04E+06	n/a	2.95E+06	1.03	n/a	n/a
Vertical Stiffener (VS)	20	8.30E+07	8.30E+07	8.07E+07	1.03	1.03	1.00
	400	5.81E+07	5.82E+07	5.65E+07	1.03	1.03	1.00
	700	1.08E+07	1.10E+07	1.05E+07	1.03	1.05	1.02
	1000	3.73E+06	3.83E+06	3.63E+06	1.03	1.05	1.03
Diagonal Tension (DT)	20	1.01E+08	1.01E+08	8.07E+07	1.25	1.25	1.00
	400	7.09E+07	7.46E+07	5.65E+07	1.25	1.32	1.05
	700	1.32E+07	1.63E+07	1.05E+07	1.25	1.55	1.24
	1000	4.56E+06	5.99E+06	3.63E+06	1.25	1.65	1.32
Diagonal Compression (DC)	20	1.49E+08	1.49E+08	8.07E+07	1.84	1.84	1.00
	400	1.04E+08	1.08E+08	5.65E+07	1.84	1.90	1.03
	700	1.93E+07	2.29E+07	1.05E+07	1.84	2.18	1.18
	1000	6.69E+06	8.77E+06	3.63E+06	1.84	2.42	1.31

of 3.0 was chosen for the web plate with $a/D = 3.0$. The acceptance criteria was based on the percent error coupled with the required computational effort.

4. Elastic critical shear buckling

Table 2 documents the elastic critical shear buckling stress, τ_{cr}, results from an eigenvalue extraction analysis conducted for the four FE models with the web at the following temperatures: 20°C, 400°C, 700°C, and 1000°C. To study the effect of the stiffener temperature, the stiffener was assumed to be either unprotected (UP) and the temperature equaled that of the web, or protected (P) by keeping the temperature of the stiffener at 20°C.

A true stiffener could not be designed to stay at 20°C while the rest of the web plate is heated due to heat conduction between the stiffener and the web plate. This is a complicated problem to model, and it was determined to adopt the idealized representation to determine whether providing insulation to the stiffener alone was an effective means of improving the web shear buckling capacity at elevated temperatures. If significant postbuckling strength at high temperatures could be achieved with an idealized insulated stiffener, this would then warrant a closer look at the insulated stiffener subjected to a more complicated (and more realistic) temperature loading.

The models discussed in Table 2 refer to those shown in Fig. 3. The NS model serves as a baseline case for weighing the benefits of providing a vertical or diagonal intermediate stiffener. The FE values are compared with the theoretical (TH) values calculated from Equation (2). The TH value of τ_{cr} reported in Table 2 for the DC and DT models assumes $a/D = 1.5$ to evaluate the applicability of the theoretical equation to a design with diagonal stiffeners.

The performance ratios listed in Table 2 compare the FE results with respect to the theoretical results (UP/TH and P/TH ratios). As expected, the theoretical model correlates well with the FE models with vertical or no stiffeners (VS and NS models, respectively). The theoretical model, however, does not predict well the behavior of webs with diagonal stiffeners. Equation (2) requires the span-to-depth ratio (a/D) as an input, however for the diagonal stiffener models this ratio cannot be directly interpreted. Should diagonal stiffeners be used to provide web support, Equation (2) must be re-formulated to account for this new geometry.

The P/UP ratio compares the FE τ_{cr} values when the stiffener is protected or unprotected. The purpose of this ratio is to quantify the benefit of offering thermal insulation solely for the stiffener. From Table 2, it can be seen that the benefit of keeping the stiffener thermally insulated for the VS model is not significant. For the DT and DC models, keeping the stiffener at 20°C has an effect for temperatures above 700°C.

The next section will focus on the postbuckling shear strength of each of the models. A comparison of stiffener orientations will be made in Section 6.

5. Postbuckling behavior

The results from the eigenvalue extraction analysis are a necessary input to initiate the nonlinear postbuckling analysis. For the postbuckling analysis to advance beyond the bifurcation point that would exist in a perfectly flat plate (as is initially modeled), a geometric imperfection must be introduced to perturb this initially "perfect" plate geometry. Typically, a small scale of the buckling mode shape associated with the lowest positive eigenvalue is used as the initial geometric imperfection [7]. In the literature, there is reference to the possibility of using a linear superposition of multiple buckling mode shapes to construct an initial geometric imperfection when there are closely-spaced eigenvalues [7]. This problem was not encountered in the current work and thus a single buckling mode shape was determined to be sufficient for the geometric imperfection.

Previous work has suggested using a scale factor of $0.001*t_w$, where t_w is the thickness of the web. This scale factor was found to be sufficient for axial compression in steel girder beams at elevated temperature [21. A maximum imperfection magnitude of $D/100$ is permitted by the *Bridge Welding Code* [4, 26], where D is the depth of the plate. The current study employed an imperfection magnitude of $D/10{,}000$ since it was found to be sufficient for advancing the nonlinear solver towards the FE value of the ultimate shear buckling strength. This scale factor is also consistent with previous work studying the web shear buckling mechanism [24].

Table 3 documents the ultimate shear buckling stress, τ_u, results for the four models at 20°C, 400°C, 700°C, and 1000°C. The theoretical (TH) value of τ_u was computed using Equation (1). As before, the DT and DC models assume $a/D = 1.5$. The UP/TH and P/TH ratios quantify the performance of the FE models with an

unprotected or protected stiffener by dividing the FE τ_u value by the TH value. When these ratios are greater than unity, this implies that the theoretical model predicts a more conservative (thus lower) ultimate shear buckling stress than the FE model.

In most cases, the theoretical model is shown to be conservative with respect to the FE model, and in general it is not a good predictor for any of the models. For the DT model at 400°C and 1000°C, however, the FE τ_u value is actually lower than the theoretical value, implying that the theoretical model predicts an unconservative value.

The P/UP ratio, which quantifies the increase in the ultimate shear buckling stress when the stiffener is protected (thermally insulated) from higher temperatures, was reported for the four FE models in Table 3. A value greater than unity implies that there is an increase in τ_u when the stiffener is protected (held at 20°C) while the rest of the web plate is heated to 400°C, 700°C, and 1000°C. Almost all of the cases reported in Table 3 have P/UP values that do not significantly differ from unity. This indicates that a protected stiffener does not greatly enhance the postbuckling shear strength at elevated temperatures. The only significant effect on τ_u is seen for the DC model at 700°C and 1000°C.

6. Comparison of stiffeners

The general conclusion from the P/UP values in Tables 2 and 3 is that protecting the stiffener does not significantly enhance the shear strength, thus the comparisons of the different stiffener performances in this section will focus only on unprotected cases. Table 4 shows ratios of the FE model results that were created to compare how one model performs with respect to another. The first three ratios listed in Table 4 quantify the performance of each of the stiffener models (VS, DT, and DC) with respect to the web plate with no intermediate stiffener (NS). The DT/VS and DC/VS ratios quantify the performance of the two diagonal stiffener models compared to the vertical stiffener model. The last ratio, DC/DT, compares the performance of the two diagonal stiffener models with respect to each other.

The τ_{cr} ratio results indicate that the DC model offers the best performance regarding the predicted elastic critical shear buckling stress. For example, the DC model offers more than double the elastic critical shear buckling stress capacity of the NS model. The VS and DT models offer increases of 1.23 and 1.50, respectively. The DC model predicts a τ_{cr} value that is approximately 1.8 times that of the VS model and 1.5 times that of the DT model, which again confirms the superior performance of the stiffener oriented in the direction of the compressive stresses.

The τ_u ratio results, however, depict a different story from the τ_{cr} ratio results. When it comes to the postbuckling shear strength, the DT/VS τ_u ratio indicates that for all temperatures, the VS model actually outperforms the DT model as indicated by the ratio values that are less than 1.0. This implies that the τ_u value predicted for the DT model is actually lower than for

Table 3
Temperature dependent ultimate shear buckling stress, τ_u, values and performance ratios for the four FE models studied

Model	T (°C)	τ_{cr} (N/m^2)			Performance ratios		
		FE model		Theoretical (TH)	FE vs. TH		P vs. UP
		UP	P		UP/TH	P/TH	P/UP
No Stiffener (NS) $a/D = 3.0$	20	1.23E+08	n/a	9.20E+07	1.34	n/a	n/a
	400	8.28E+07	n/a	7.55E+07	1.10	n/a	n/a
	700	2.19E+07	n/a	1.57E+07	1.40	n/a	n/a
	1000	4.03E+06	n/a	3.95E+06	1.02	n/a	n/a
Vertical Stiffener (VS)	20	1.42E+08	1.42E+08	1.05E+08	1.36	1.36	1.00
	400	1.14E+08	1.19E+08	8.43E+07	1.36	1.42	1.04
	700	2.42E+07	2.84E+07	1.73E+07	1.40	1.64	1.17
	1000	5.02E+06	5.11E+06	4.52E+06	1.11	1.13	1.02
Diagonal Tension (DT)	20	1.24E+08	1.24E+08	1.05E+08	1.18	1.18	1.00
	400	7.24E+07	7.37E+07	8.43E+07	0.86	0.87	1.02
	700	2.24E+07	2.46E+07	1.73E+07	1.29	1.42	1.10
	1000	4.36E+06	5.36E+06	4.52E+06	0.96	1.18	1.23
Diagonal Compression (DC)	20	1.72E+08	1.72E+08	1.05E+08	1.64	1.64	1.00
	400	1.01E+08	1.09E+08	8.43E+07	1.20	1.29	1.08
	700	1.96E+07	2.91E+07	1.73E+07	1.14	1.68	1.48
	1000	5.41E+06	7.30E+06	4.52E+06	1.20	1.61	1.35

Table 4
Performance ratios for to compare the different FE models

Ratio of FE model results	T (°C)	τ_{cr} ratio	τ_u ratio	Ratio of FE model results	T (°C)	τ_{cr} ratio	τ_u ratio
VS/NS	20	1.23	1.16	DT/VS	20	1.22	0.87
	400	1.23	1.38		400	1.22	0.63
	700	1.23	1.11		700	1.22	0.92
	1000	1.23	1.25		1000	1.22	0.87
DT/NS	20	1.50	1.01	DC/VS	20	1.79	1.21
	400	1.50	0.87		400	1.79	0.88
	700	1.50	1.02		700	1.79	0.81
	1000	1.50	1.08		1000	1.79	1.08
DC/NS	20	2.20	1.40	DC/DT	20	1.47	1.39
	400	2.20	1.22		400	1.47	1.39
	700	2.20	0.90		700	1.47	0.88
	1000	2.20	1.34		1000	1.47	1.24

the VS model. For the DC model, the DC/VS τ_u ratios are less than unity for 400°C and 700°C; at 20°C and 1000°C, the DC model offers a modest increase in ultimate shear buckling stress capacity as compared to the VS model.

The primary conclusion from the results presented in Table 4 is that, despite the promising τ_{cr} ratios, the τ_u ratios suggest that the DT model offers no improvement in the postbuckling shear strength compared to the VS model, while the DC model offers only modest improvement at certain temperatures. Given the complexity of attaching a diagonal stiffener, it appears that the vertical stiffener is the better option when selecting an intermediate stiffener.

One of the primary motivations for investigating diagonal orientations of the stiffeners was to further probe the mechanics of web shear buckling. Of particular interest was the contribution of the compressive stresses to the postbuckling shear strength of the web plate. Employing diagonal stiffeners in both the tension field and compressive stresses directions offered an opportunity to further explore the hypothesized contributions of the compressive stresses in the postbuckling range. The τ_u ratio of 1.21 for DC/VS at 20°C in Table 4 indicates that the DC model offered some increase in the ultimate shear buckling stress capacity. This observation suggests that the contribution of compressive stresses to the postbuckling shear strength is something to be more closely investigated for any future analytical models.

7. Conclusions and future work

The primary goal of this paper was to determine how postbuckling shear performance of a steel plate girder could be improved at high temperatures by examining two parameters: the temperature and the orientation of the vertical stiffener. One set of analyses assumed that the stiffener reached the same temperature as the web in a fire, and another set of analyses assumed that the stiffener stayed at ambient temperature (presumably through some fire protection). Although this last scenario is not realistic given the conductivity of steel, it forms an envelope (upper bound solution) for evaluation. It was found that providing thermal protection for the stiffeners alone has a minimal beneficial effect on the ultimate shear buckling strength, τ_u, and therefore is not recommended for improving the postbuckling shear strength of webs at elevated temperatures.

In the stiffener orientation study, it was found that placing the stiffener along the diagonal of the tensile stresses does not offer any advantage for the postbuckling strength. Placing the stiffener along the diagonal of the compressive stresses offers some advantage at certain temperatures compared to a vertical stiffener. However, attaching a diagonal stiffener to the web is complex, and the advantage for strength is inconsistent (depending on the temperature) and not significant enough to recommend this design.

In the context of understanding the behavior of shear buckling, the diagonal stiffener in the compressive direction does affect τ_u, albeit not more than 20%, and therefore suggests that the contribution of compressive stresses to the postbuckling shear strength, which is typically ignored, is something to be more closely investigated in future studies.

Acknowlegments

This research was made with Government support under and awarded by DoD, Air Force Office of Scientific Research, National Defense Science and

Engineering Graduate (NDSEG) Fellowship, 32 CFR 168a, provided to Mr. Glassman. This research was also sponsored by the National Science Foundation (NSF) under grant CMMI-1068252. All opinions, findings, and conclusions expressed in this paper are of the authors and do not necessarily reflect the policies and views of the sponsors.

References

[1] American Institute of Steel Construction (AISC). Steel Construction Manual (13th ed.) 2005.

[2] American Institute of Steel Construction (AISC). Steel Bridge Design Handbook [online]. Available: http://www.aisc.org/contentNSBA.aspx?id=20244. [Accessed 21 December 2012].

[3] American Association of State Highway and Transportation Officials. AASHTO LRFD Bridge Design Specifications (5th ed.) with 2010 Interim revisions [online]. Available: http://www.knovel.com/knovel2/Toc.jsp?BookID=4852. [Accessed 22 December 2012].

[4] AASHTO/AWS (American Association of State Highway and Transportation Officials/American Welding Society). Bridge Welding Code, D1.5M/D1.5. 2002.

[5] Basler K. Strength of Plate Girders in Shear. Trans ASCE. 1961;128(2).

[6] Chung P. (ed.), Wolfe, R. (ed.), Ostrom, T. (ed.), Hida, S. (ed.). Accelerated bridge construction applications in California – a lessons learned report. USA: California Department of Transportation (CALTRANS). 2008.

[7] Dassault Systemes. 2011. Abaqus 6.11ef Online Documentation. Accessed August 16, 2012.

[8] European Committee for Standardization (CEN). Eurocode 1: Actions on Structures – Part 1-2: General Actions – Actions on Structures Exposed to Fire. Brussels: CEN. 2002.

[9] European Committee for Standardization (CEN). Eurocode 3: Design of Steel Structures – Part 1-2: General Rules – Structural Fire Design. Brussels: CEN. 2005.

[10] Garlock M, Payá-Zaforteza I, Kodur V. Fire Hazard in Bridges: Review, Assessment and Repair Strategies. Engineering Structures. 2012;35:89-98.

[11] Iqbal N, Salley MH, Weerakkody S. Fire Dynamics Tools (FDTs) Quantitative Fire Hazard Analysis Methods for the U.S. Nuclear Regulatory Commission Fire Protection Inspection Program (NUREG-1805). Washington: GPO. 2004.

[12] Lee S, Davidson J, Yoo C. Shear Buckling Coefficients of Plate Girder Web Panels. Computers and Structures. 1996;59(5): 789-95.

[13] Lee SC, Yoo CH. Strength of Plate Girder Web Panels Under Pure Shear. Journal of Structural Engineering. 1998;124(2): 184-94.

[14] Lee SC, Lee DS, Yoo CH. Ultimate shear strength of long web panels. Journal of Constructional Steel Research. 2008;64:1357-65.

[15] Marsh C, Ajam W, Ha H-K. Finite Element Analysis of Postbuckled Shear Webs. Journal of Structural Engineering. 1988;114(7):1571-87.

[16] Mudan KS. Thermal Radiation Hazards from Hydrocarbon Pool Fires. Progress in energy and Combustion Science. 1984;10:59-80.

[17] National Fire Protection Association (NFPA). Standard for Road Tunnels, Bridges, and Other Limited Access Highways. 2008.

[18] Rahal KN, Harding JE. Transversely stiffened girder webs subjected to shear loading – part 1: Behaviour. Proceedings of the Institution of Civil Engineers. 1990a;89(2):47-65.

[19] Rahal KN, Harding JE. Transversely stiffened girder webs subjected to shear loading – part 2: Stiffener design. Proceedings of the Institution of Civil Engineers. 1990b;89(2):67-87.

[20] Schiffner DC. Analysis of Collapsed Alabama Bridge due to Fire (M.S. Thesis). Princeton: Princeton University. 2011.

[21] Selamet S, Garlock ME. Predicting the maximum compressive beam axial force during fire considering local buckling. Journal of Constructional Steel Research. 2012;71:189-201.

[22] Timoshenko SP, Gere JM. Theory of Elastic Stability (2nd ed.). New York: McGraw-Hill Book Company, Inc. 1961.

[23] Vimonsatit V, Tan K-H, Ting S-K. Shear strength of plate girder web panel at elevated temperature. Journal of Constructional Steel Research. 2007a;63:1442-51.

[24] Vimonsatit V, Tan K-H, Qian Z-H. Testing of Plate Girder Web Panel Loaded in Shear at Elevated Temperature. Journal of Structural Engineering. 2007b;133(6):815-24.

[25] Wagner H. Flat Sheet Metal Girder with Very Thin Metal Web. Tech Notes 604, 605, 606. Washington: National Advisory Committee on Aeronautics. 1931.

[26] Yoo CH, Lee SC. Mechanics of Web Panel Postbuckling Behavior in Shear. Journal of Structural Engineering. 2006;132(1):1580-9.

[27] Ziemian RD. Guide to Stability Design Criteria for Metal Structures, 6th ed. Hoboken: John Wiley & Sons. 2010.